Materials Today Communications 37 (2023) 107461

Contents lists available at ScienceDirect

Materials Today Communications

journal homepage: www.elsevier.com/locate/mtcomm

The effect of accretion temperature on microstructure and bending strength of atmospheric ice

C. Fallon [a,*], E. Truyen [b], D. Eakins [b], H. Pervier [c], M.L.A. Pervier [c], M. Aceves Lopez [b]

[a] Department of Mechanical Engineering, University of Bath, Bath, BA2 7AY, UK
[b] Department of Engineering Science, University of Oxford, Oxford, OX1 3PJ, UK
[c] Cranfield University, Cranfield, MK43 0AL, UK

ARTICLE INFO

Keywords:
Ice
Atmospheric
Rime
Glaze
Bending
Flexure

ABSTRACT

Accurate determination of the mechanical response of atmospheric ice is key to understanding the risks associated with ice impact on aircraft during flight. Two types of atmospheric ice which are of particular interest to the aerospace industry are studied. Rime and Glaze ice are each manufactured in an icing wind tunnel facility under controlled conditions. Rime ice is accreted at a temperature of −20 °C, and Glaze ice is accreted at −5 °C. Quasi-static three-point bend tests are performed on both types of ice to understand the effect of accretion temperature, and therefore microstructure, on strength. The results indicate that the ice accretion temperature, and thus microstructure, has a significant influence on the bending strength. On average, the bending strength of Rime ice is 9.0 ± 0.18 MPa compared to 4.4 ± 0.093 MPa for Glaze. The comparatively lower accretion temperature of Rime results in smaller grain sizes and higher bending strength. In contrast, the effective modulus appears insensitive to ice microstructure, with an average value of 3.5 ± 0.12 GPa for Rime compared to 3.6 ± 0.098 GPa for Glaze. Furthermore, the results indicate that both the bending strength and effective modulus are insensitive to the ice storage time.

1. Introduction

Accurate prediction of the deformation and failure of components subjected to impact with ice is of great interest to the aerospace industry. During flight, aircraft components may be subjected to high velocity ice impact either due to adverse weather conditions, or due to the ingestion of ice that has accreted on the leading edge of exposed components such as fan blades. This can lead to wear and loss of fatigue life of downrange components, or in the worst case, failure and loss of performance [1]. Thus, it is of the utmost importance that aircraft components are designed to withstand the stresses associated with this threat.

Ice can adopt a large number of crystalline structures or amorphous states [2]. One of these forms, ice Ih, possesses a hexagonal crystal structure and is stable at ambient pressures [2]. Ice Ih is often referred to as ordinary ice and is the common terrestrial form [2], presenting in nature as, for example, glacier ice, floating sheet ice, hailstones and atmospheric ice [3]. The microstructure and resulting mechanical properties can be affected by various factors during formation such as temperature, water flow and impurities which influence both the size and shape of ice grains. Atmospheric ice, the subject of this study, is formed when supercooled water droplets hit a cold surface and freeze upon contact. Depending on the meteorological conditions, different types of atmospheric ice can be obtained, for example, Rime ice and Glaze ice [3]. In this study, Rime ice is accreted at a temperature of −20 °C, whereas Glaze ice is accreted at −5 °C.

A first step towards understanding the mechanical behaviour of this atmospheric ice is to characterise its quasi-static response. There has already been some effort in the literature dedicated to understanding the compressive and tensile behaviour at quasi-static strain-rates [2,4–8] of both single crystal and polycrystalline ice varieties.

In Petrovic's [9] review paper on the mechanical properties of ice, some typical values for the strength and elastic properties of ice are reported. Over the temperature range −10 °C to −20 °C, the compressive strength of ice typically ranges between 5 and 25 MPa. As is the case for other brittle materials, it is understood that ice is weaker in tension than compression. Petrovic [9] reports that over the temperature range −10 °C to −20 °C, the tensile strength of ice ranges between 0.7 and 3.1 MPa. In terms of Young's modulus, values in the range 9.7–11.2 MPa are typically reported for polycrystalline ice at a temperature of −10 °C, with a Poisson's ratio in the range 0.29–0.32 [9]. There is obvious scatter in the literature data, which is no doubt due to the dependence of ice's

* Corresponding author.
E-mail address: cf771@bath.ac.uk (C. Fallon).

https://doi.org/10.1016/j.mtcomm.2023.107461
Received 22 June 2023; Received in revised form 11 October 2023; Accepted 28 October 2023
Available online 31 October 2023

mechanical response on a number of variables including temperature, strain-rate, tested volume and grain size [9].

Strain-rate dependence is a key factor in characterising the mechanical response of ice. Schulson [4] noted that the compressive strength is sensitive to strain-rate, reporting that a ductile to brittle transition occurs at a strain-rate $\sim 10^{-3}$ s^{-1} at test temperatures of −10 °C. Mapping the strain-rate space between 10^{-8} s^{-1} and 10^{-3} s^{-1}, they report a trend of increasing compressive strength from around 0.5 MPa at 10^{-8} s^{-1} to 9 MPa at 10^{-3} s^{-1} for ice Ih with ∼ 1 mm grain size. This is followed by a reduction in compressive strength to about 6 MPa at 10^{-1} s^{-1}, albeit with considerable scatter in the data. Interestingly, Schulson [4] reported that the tensile strength is relatively insensitive to strain-rate over the range 10^{-7} s^{-1} to 10^{-3} s^{-1}, but that a ductile to brittle transition does occur, but at lower strain-rates compared to that observed in compression [2].

Temperature dependence also has an important role to play. Haynes [5] showed that the compressive response of polycrystalline snow-ice is strongly dependent on test temperature, reporting for one series of tests an average compressive strength increase from 4.9 MPa at −0.1 °C to 40.1 MPa at −53 °C. Conversely, the tensile strength was shown to be only weakly dependent on temperature, varying between 1.7 and 3.2 MPa over the range 0 °C to −40 °C. Once more, there is significant scatter in the data which the authors attribute to challenges associated with performing tensile tests on ice, for example, slippage of the specimen in the gripping system [5].

A few authors have also reported on sensitivity to grain size and test specimen volume. Currier and Schulson [8] conducted tensile experiments on equiaxed and randomly orientated polycrystalline ice and reported that the fracture strength of ice decreases as the grain diameter increases (for tests at a strain-rate of 10^{-6} s^{-1}, at a temperature of −10 °C). Their analysis suggests that the strength is controlled by microcrack propagation, nucleated through dislocation pile-ups at grain boundaries. The response is described using a Hall-Petch relationship. Further, the tensile response has also been shown to be influenced by specimen test volume. In a study by Dempsey et al. [6,7], the authors reported a significant size effect, with the tensile strength of ice decreasing with increasing specimen size. Aly et al. [10] reached a similar conclusion. They conducted a comprehensive literature study on the scale effect in ice flexural strength, reporting a considerable decrease in flexural strength as the specimen size increased for both freshwater and sea ice.

There are, however, very few studies examining the mechanical response of atmospheric ice in particular [11–15]. Some work exists on the adhesion of atmospheric ice, specifically with a view to the design of de-icing and anti-icing aircraft systems. This work tends to focus on experimental rig design and modelling for the measurement and prediction of adhesion strength [11,16–19]. There is significant scatter in the reported values but most results fall in the range between 50 and 500 kPa for adhesive shear strength [19].

Early work by Druez et al. [11] examined the compressive response of atmospheric ice accumulated at various temperatures and air speeds. Later, Kermani et al. [12] reported compressive tests on atmospheric ice at a range of strain-rates $\sim 10^{-5}$ s^{-1} to 10^{-2} s^{-1}. The ice was accumulated in a wind tunnel at a liquid water content (LWC) of 2.5 g m^{-3}, a wind speed of 10 m s^{-1} and at various temperatures. It was established that the compressive strength increased as the test temperature decreased and that at low strain-rates ($\sim < 10^{-2}$ s^{-1}), the compressive strength increased with decreasing accumulation temperature, owing to a reduction in grain size. Of particular relevance to the present study, Kermani et al. [13] then investigated the flexural response of different types of atmospheric ice, accumulated at a LWC of 2.5 g m^{-3} and a wind speed of 10 m s^{-1}. Three-point bend tests were performed at strain-rates in the range $\sim 10^{-5}$ s^{-1} to 10^{-2} s^{-1}. The results displayed a clear dependence on accumulation and testing temperatures. At a strain-rate of 2×10^{-3} s^{-1}, an accumulation temperature of −10 °C and a test temperature of −3 °C, the authors measured an average flexural strength of 2.74 ± 0.59 MPa and an average effective modulus of 1.01 ± 0.18 GPa.

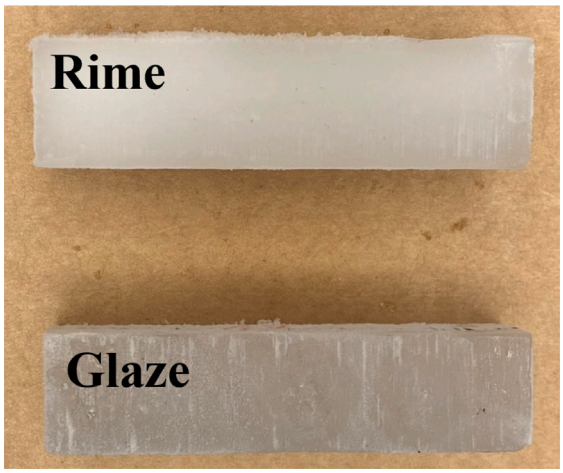

Fig. 1. Photograph of typical Rime ice and Glaze ice specimens; 60 mm in length and 15 mm by 15 mm in cross-section.

Reviewing the literature illustrates the challenges faced in understanding and characterising the mechanical response of ice, and in particular, atmospheric ice. Significant scatter in the literature data persists, perhaps due to the experimental challenges involved but also due to the ice mechanical response dependence on a number of variables including strain-rate, temperature and test volume.

In this work, we take the first step towards understanding the mechanical response of two different types of atmospheric ice which are of particular relevance to the aircraft industry [3]. The flexural response of Rime and Glaze ice will be studied. This is key to assessing the threat of ice loading on aircraft structures [20,21]. As described by Han et al. [20] in their work on ice impact fragmentation in aircraft engines, accreted ice is typically slender in geometry, and thus in their model of ice brittle solid fragmentation, inspired by Croasdale [21], it is the ice flexural strength which is used as the failure criterion [20,21]. There however remains a lack of understanding of how the differing microstructures of Rime and Glaze ice affect the resulting mechanical properties. In this work, we will present the experimental results from a series of quasi-static three-point bend tests, considering the effect of two variables: (i) the ice accretion temperature *i.e.* Rime *vs.* Glaze and (ii) the ice storage time *i.e.* the time from ice production to test in order to establish if storage duration plays a role in the mechanical response.

2. Ice specimens

Two different types of atmospheric ice are studied: Rime and Glaze. Supercooled water droplets are accreted onto cold, aluminium plates, positioned perpendicular to the incoming flow, in an icing wind tunnel facility at Cranfield University, where various meteorological conditions can be simulated. For both ice types, the wind tunnel speed was 50 m s^{-1}, the cloud liquid water content (LWC) was 0.4 g m^{-3} and the droplet median volume diameter was 20 μm. Glaze ice was produced at a temperature of −5 °C whereas Rime ice was produced at a temperature of −20 °C. Since Glaze ice is manufactured at a comparatively lower freezing rate, there is sufficient time for air to escape during the freezing process resulting in a transparent appearance. Conversely, Rime ice is produced by rapid freezing which results in trapped air bubbles giving Rime ice its characteristic cloudy appearance. Typical Rime and Glaze ice specimens are pictured in Fig. 1.

Fig. 2 presents micrographs of Rime and Glaze ice specimens, obtained using a replica technique, first reported by Pervier et al. [22]. A layer of nail varnish is applied to the surface of interest and after

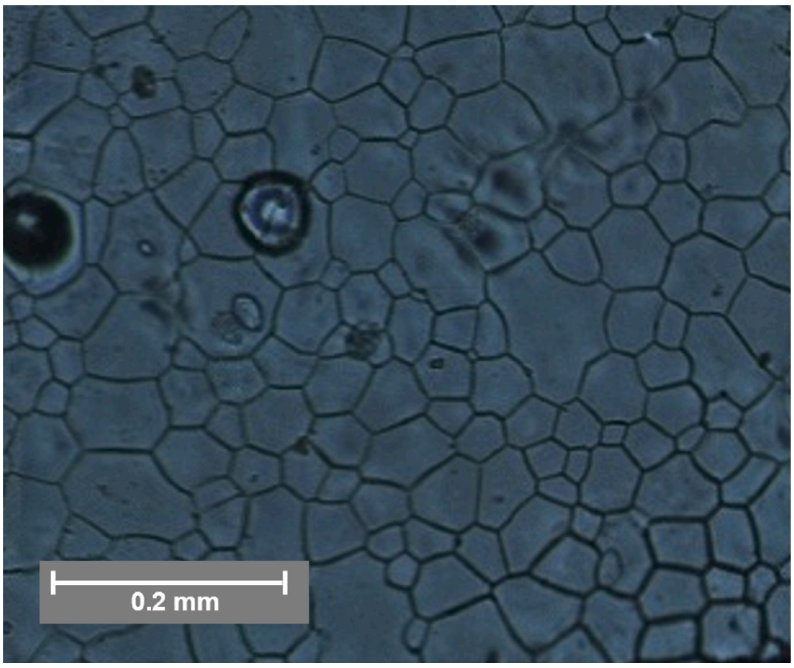

(a)

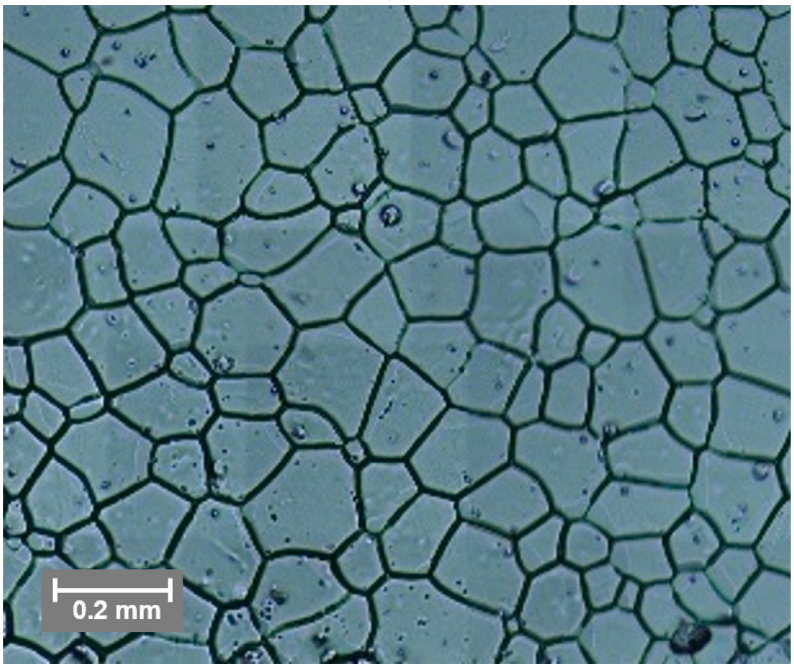

(b)

Fig. 2. Optical micrographs of (a) Rime ice and (b) Glaze ice, taken at the interface using a replicate technique [22].

a drying time of 24 hours, the nail varnish layer is peeled off the ice giving a replica of the ice surface. The images suggest the presence of air bubbles for the Rime ice specimen, approximately 10 μm in diameter, particularly at the grain boundaries. Most obvious however is the discrepancy in grain size between the specimens, with Rime ice exhibiting grain sizes significantly smaller than Glaze ice. After taking a series of photos of the replica through a microscope and stitching them together, the average grain size was obtained by using the mean linear intercept method on ten measurements taken in different directions. On each micrograph, a line of known length is drawn and the number of grains intersected by this line is counted. The average grain size is obtained by dividing the line's length by the number of grains. The average grain size for Rime is measured to be approximately 50 μm compared to 110 μm for Glaze.

The ice is machined in a cold room into prisms, nominally 20×20 mm in cross-section and 130 mm in length. The ice is stored in a −50 °C freezer until the time of the experiment. The microstructure of the ice is monitored using the replica technique described previously to verify that the microstructure, and thus grain size remains relatively constant when stored at −50 °C. Prior to the test, the ice is then transferred to the experimental room where it is stored in a cool box in a −20 °C freezer for a few hours to prevent thermal shock. The ice specimens are removed from this freezer, positioned on the test rig and loaded to failure in less than a minute. The test rig supports were also cooled

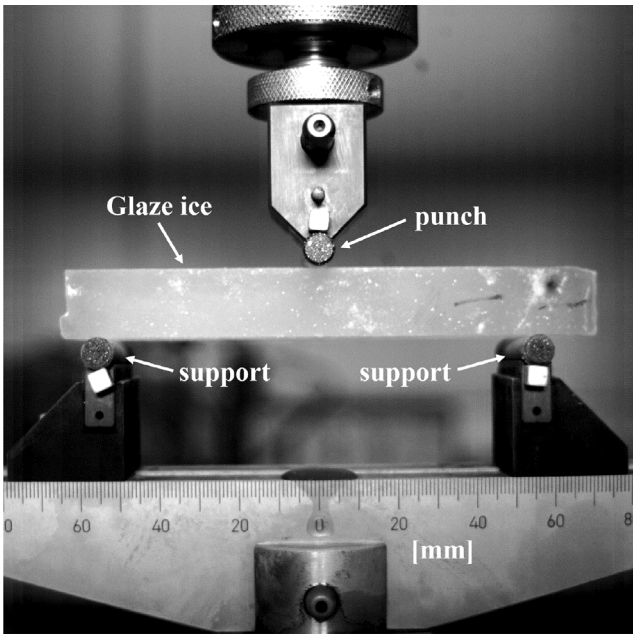

Fig. 3. Photograph of the three-point bend test set-up on a screw-driven Instron testing machine showing a Glaze ice specimen prior to a test.

in this −20 °C freezer between tests to minimise heat loss and prevent melting at the contact points.

3. Experimental methodology

An Instron screw-driven testing machine was used to perform the three-point bend tests. Fig. 3 illustrates how the ice specimens were loaded onto the three-point bend rig such that the supported length, $L = 120$ mm. In all tests, the interface face is face down and the applied force is in the direction opposite to the growth direction. The supports and puncher were 40 mm long cylinders with a diameter of 8 mm. The puncher was displacement-controlled at a rate of $\dot{\delta} = 0.24$ mm s^{-1}. This corresponds to a nominal strain-rate of 2×10^{-3} s^{-1} as calculated from simple elastic beam theory [23],

$$\dot{\epsilon} = \frac{6\,h\,\dot{\delta}}{L^2} \tag{1}$$

where h is the height of the specimen.

4. Results

Fig. 4 presents the force–displacement plots recorded during the three-point bend tests for Rime and Glaze ice specimens after 0, 5 and 10 days of storage in a −50 °C freezer. The plots illustrate that the results are relatively consistent and reveal two significant insights.

Firstly, the gradients of the force–displacement plots appear consistent between Rime and Glaze ice. The gradient of these plots, F/d, can be used to obtain an expression for the effective modulus, E_f according to Eq. (2), obtained from simple elastic beam theory [23]. The form of the force–displacement curves suggests that, after some settling-in, this assumption is reasonable. All variables are as that defined previously, and w is the width of the specimen.

$$E_f = \frac{1}{4\,w}\frac{L^3}{h^3}\frac{F}{d} \tag{2}$$

The gradient, F/d for each specimen was estimated from the linear portion of the response. Each experiment is repeated at least three times and the average, or mean, effective modulus, E_f is tabulated in Table 1 alongside the standard deviation of the mean. It appears that E_f is

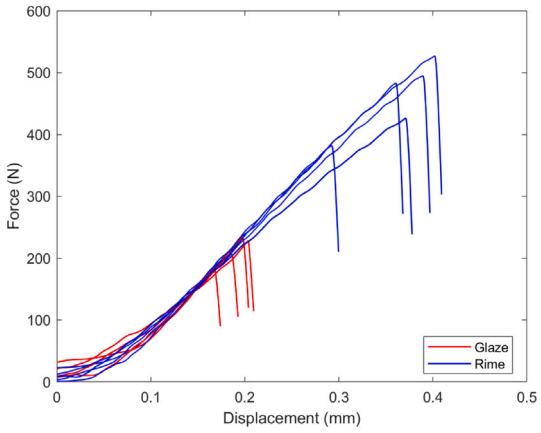

(a) 0 days

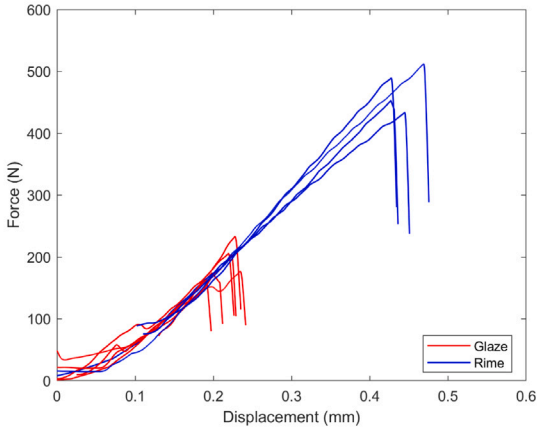

(b) 5 days

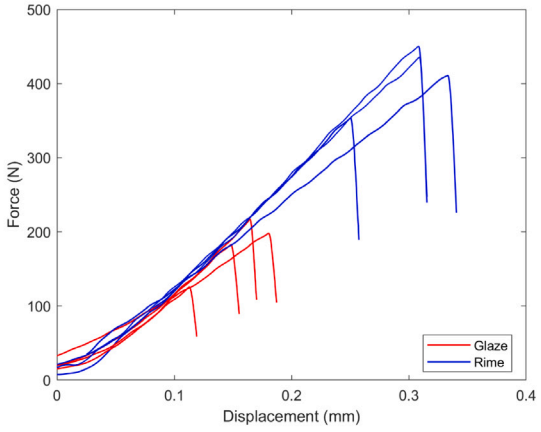

(c) 10 days

Fig. 4. Three-point bend test force–displacement results at a punch rate of 0.24 mm s^{-1} for Rime and Glaze ice after a storage time of (a) 0 days, (b) 5 days and (c) 10 days.

insensitive to both storage time, and ice microstructure *i.e.* there is no discernible difference between that for Rime and Glaze ice. The overall average effective modulus, across all storage times, for all Rime samples tested was 3.5 ± 0.12 GPa and for Glaze, 3.6 ± 0.098 GPa.

Next, we examine the bending strength dependence on storage time and ice accretion temperature. Eq. (3) relates the failure load, F_{max} to the bending strength, σ_f using the principles of simple elastic beam

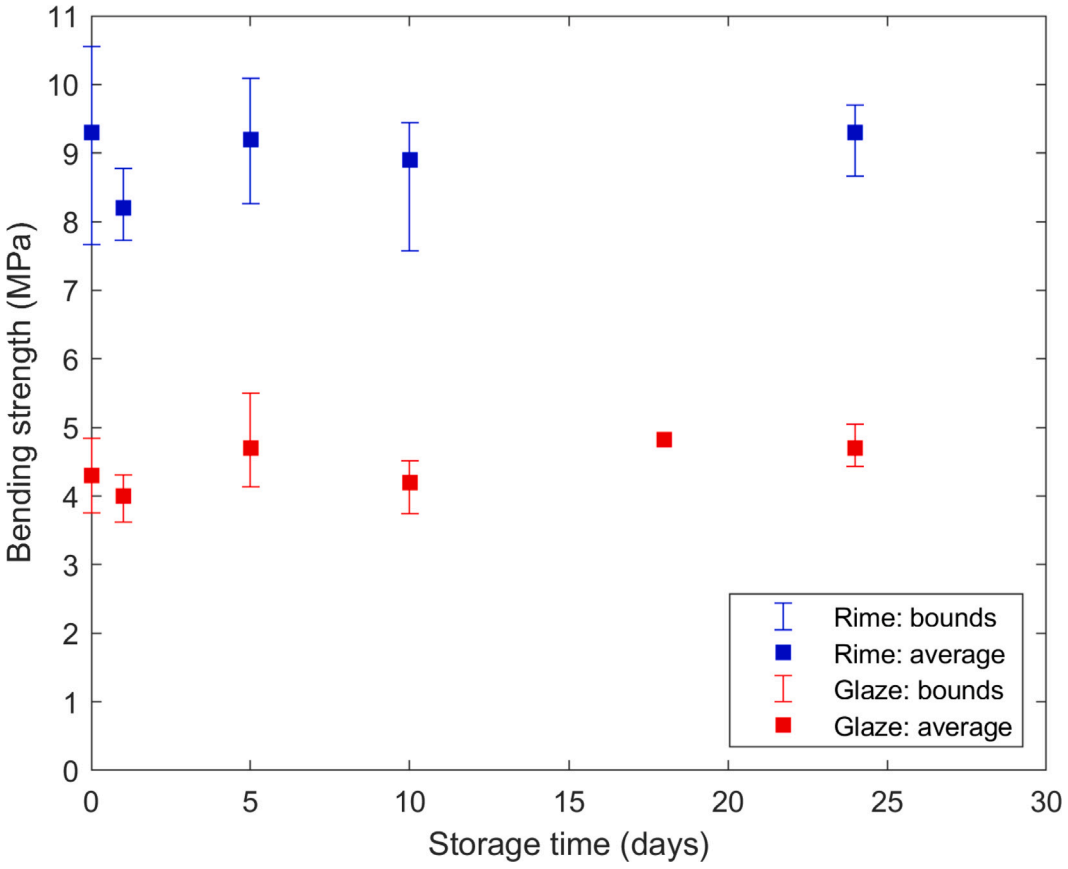

Fig. 5. Bending strength evolution with storage time for Rime and Glaze ice. The ice is stored in a −50 °C freezer until the time of the test.

Table 1
Average effective modulus, E_f according to Eq. (2) for Rime and Glaze ice after a variety of storage durations.

Storage time (days)	Effective modulus (GPa)	
	Glaze	Rime
0	3.5 ± 0.21	3.4 ± 0.13
1	3.4 ± 0.14	3.1 ± 0.13
5	3.7 ± 0.29	2.9 ± 0.13
10	3.5 ± 0.19	3.7 ± 0.13
24	3.7 ± 0.27	4.4 ± 0.03

bending [23],

$$\sigma_f = \frac{3}{2}\frac{F_{max}\,L}{w\,h^2} \tag{3}$$

The bending strength variation with storage time is plotted in Fig. 5. Each experiment was repeated at least three times. The average bending strength is calculated and has been plotted in Fig. 5 with bounds extending to the maximum and minimum recorded values. Note, only one sample was tested at the 18 day storage duration and thus bounds have not been plotted for this point. It appears that for both Rime and Glaze ice, the bending strength is insensitive to the storage time, at least up to 24 days, when stored at −50 °C. This finding is useful for future researchers, who for practical reasons, may have to test ice which has undergone a storage period. This work suggests that the mechanical properties remain unchanged for these storage conditions. The microstructure of both Rime and Glaze ice remained relatively constant under these storage conditions, which may explain the insensitivity to storage duration.

Significantly, Fig. 5 illustrates that Rime ice is twice as strong in bending compared to Glaze ice across all storage durations. The overall average bending strength, across all storage times, for all Rime samples tested was 9.0 ± 0.18 MPa and for Glaze, 4.4 ± 0.093 MPa.

We postulate that the difference in bending strength between Rime and Glaze ice can be explained by examining microstructure. As discussed previously, it has been shown that the ice accretion temperature influences the grain size [3]. Previous researchers tend to broadly agree that the strength of ice in tension [3,8], compression [11,12] and flexure [13] increases with a reduction in grain size. Currier and Schulson [8] postulated that ice strength is controlled by microcrack propagation, nucleated through dislocation pile-ups at grain boundaries where microcracks and dislocation pile-ups are of lengths proportional to the grain diameter. They used a Hall Petch relationship to describe how the tensile strength of equiaxed and randomly oriented polycrystalline ice varies with grain size. We remain cautious about providing false comparisons between such literature studies and our data, where loading conditions, ice types and specimen geometries differ between studies. Nevertheless, our results match the trend reported in the literature: ice accreted at a lower temperature *i.e* Rime, has a smaller average grain size and is thus stronger in bending compared to ice accreted at a higher temperature *i.e.* Glaze.

It is interesting to note that the flexural strength values reported in this study are higher than that typically reported in the literature. One possible explanation is the relatively small specimen volume examined in our study. Aly et al. [10] conducted a comprehensive literature review on the scale effect in ice flexural strength, reporting a considerable decrease in flexural strength as the specimen size increased. Aly et al. [10] derived empirical models of freshwater and sea ice flexural strength as a function of beam volume. They postulate that with increasing specimen size, the probability of encountering a critical flaw increases, which causes a decrease in strength [10,24].

Fig. 6 illustrates how our data compares with Aly et al.'s [10] literature study (see Fig. 7 in [10] for Aly et al.'s original plot). Note,

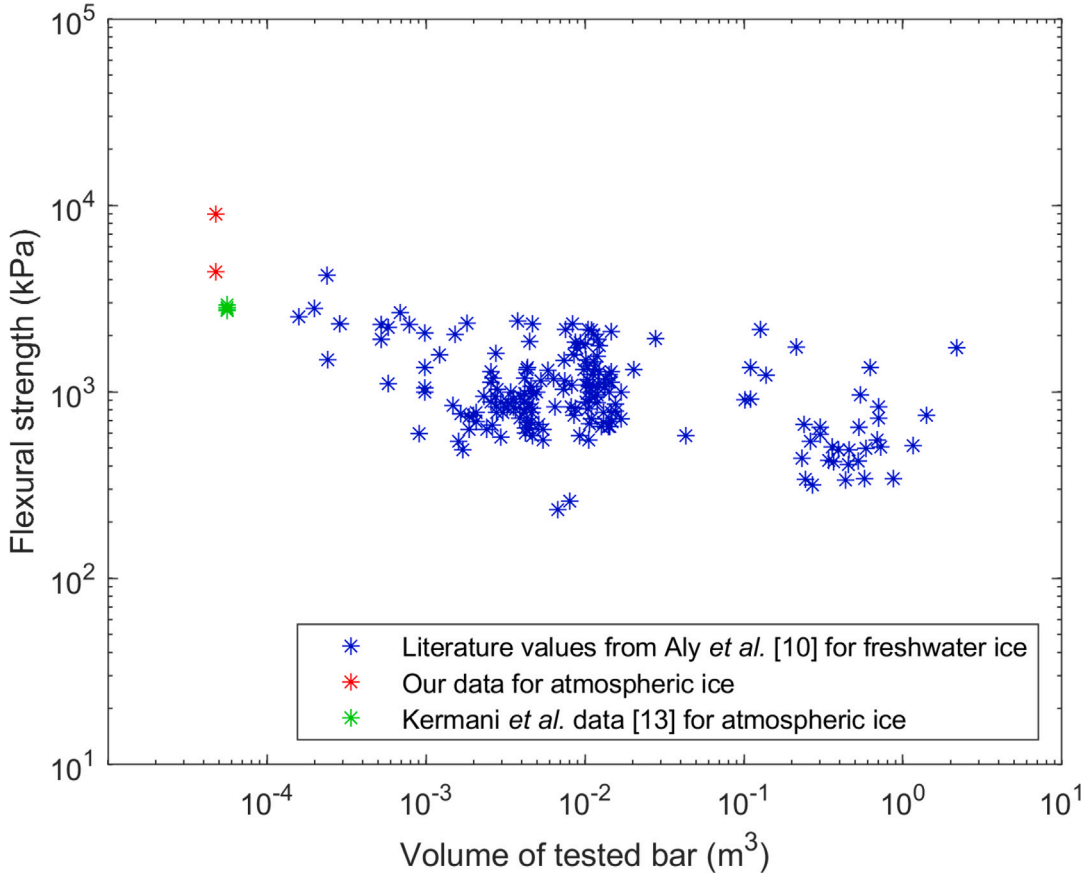

Fig. 6. Plot summarising ice flexural strength dependency on tested bar volume. Literature data points (*) are taken from Aly et al.'s [10] work examining the flexural strength of freshwater ice. Our data (*) on flexural strength of atmospheric ice is plotted. Kermani et al.'s [13] data (*) on flexural strength of atmospheric ice is also plotted.

this study by Aly et al. [10] considers freshwater ice, not atmospheric. Furthermore, Aly et al.'s [10] literature data encompasses both field and laboratory tests, and three-point and four-point bending tests.

Fig. 6 illustrates that our study has extended the previously tested domain and appears to confirm the reported trend: increasing ice flexural strength with decreasing specimen volume. On Fig. 6, we have also plotted data from Kermani et al.'s [13] study on the flexural strength of atmospheric ice for comparison. Kermani et al. [13] performed three-point bend tests on atmospheric ice at a similar strain-rate to our study and reported measured flexural strength in the range 2–2.8 MPa, depending on accretion and test temperature. This is lower than the flexural strengths reported in our study. To explain this discrepancy, we consider two contributing factors. Firstly, our icing wind tunnel conditions differ to Kermani et al.'s [13] resulting in different grain sizes. Kermani et al. [13] reported an average grain size of 1.5 mm for ice accreted at −6 °C, and 0.5 mm for ice accreted at −10 °C. These grain sizes are larger than that found in our study: Glaze ice was accreted at a temperature of −5 °C, resulting in an average grain size of 110 μm whereas Rime ice was accreted at a temperature of −20 °C resulting in an average grain size of 50 μm. We also note that the different LWC and wind tunnel speeds between this study and that of Kermani et al. [13] may contribute to the discrepancy in grain size, though this is the subject of some debate in the literature [3,25,26]. Secondly, the loading direction differs between our study and Kermani et al.'s [13]. Kermani et al.'s [13] bar is rotated by 90° about the longitudinal bar axis in comparison to our study, perhaps suggesting again that microstructural effects are at play. However, the effect of loading direction is debated in the literature [27,28] and thus the authors suggest a future study examining this variable alone to ascertain its influence.

As demonstrated, it is important to remain cautious about drawing comparisons between studies where multiple key variables, including specimen geometry, accumulation conditions and test temperature differ. In this work, we have kept constant the test conditions, specimen geometry and strain rate and have therefore identified ice accretion temperature and thus microstructure as having a key influence on the bending strength of atmospheric ice. In so doing, we have taken a first step towards understanding the mechanical response of two different types of atmospheric ice, Rime and Glaze, which are of particular relevance to the aircraft industry.

5. Conclusions

An experimental investigation was performed to ascertain the effect of: (i) ice accretion temperature and (ii) ice storage duration, on the room temperature, quasi-static, three-point bending response of two types of atmospheric ice. The ice is manufactured at an icing wind tunnel facility, at a wind tunnel speed of 50 m s^{-1}, a cloud liquid water content of 0.4 g m^{-3} and a droplet median volume diameter of 20 μm. Glaze ice was accreted at a temperature of −5 °C whereas Rime ice was accreted at −20 °C.

It is concluded that the effective modulus is insensitive to both the ice storage duration, at least up to 24 days, at a storage temperature of −50 °C, and to the ice microstructure. Across all storage times, the average effective modulus for Rime ice was 3.5 ± 0.12 GPa, compared to 3.6 ± 0.098 GPa for Glaze. The bending strength is also insensitive to the ice storage time. However, the ice accretion temperature, and thus microstructure, has a significant influence on the bending strength. Rime ice is twice as strong as Glaze ice in bending. Across all storage times, Rime ice exhibits an average bending strength of 9.0 ± 0.18 MPa compared to 4.4 ± 0.093 MPa for Glaze ice. The difference in flexural strength is attributed to a microstructural effect where Rime ice exhibited an average grain size of 50 μm, smaller than the average grain size of Glaze, 110 μm.

CRediT authorship contribution statement

C. Fallon: Conceptualization, Investigation, Formal analysis, Visualization, Writing – original draft, Writing – review & editing. **E. Truyen:** Conceptualization, Investigation, Formal analysis, Writing – review & editing. **D. Eakins:** Supervision, Writing – review & editing. **H. Pervier:** Investigation. **M.L.A. Pervier:** Investigation, Writing – review & editing. **M. Aceves Lopez:** Investigation.

Declaration of competing interest

The authors declare the following financial interests/personal relationships which may be considered as potential competing interests: Daniel Eakins reports financial support was provided by Innovate UK.

Data availability

Data will be made available on request.

Acknowledgements

The authors are grateful to Peter West at Cranfield University for the ice manufacture. We are also grateful to Rolls-Royce plc, Aerospace Technology Institute and Innovate UK (113155) for their financial support.

References

[1] J.G. Mason, W. Strapp, P. Chow, The ice particle threat to engines in flight, in: 44th AIAA Aerospace Sciences Meeting and Exhibit, Reno, Nevada, 2006.
[2] E.M. Schulson, The structure and mechanical behavior of ice, J. Miner. Met. Mater. Soc. 51 (2) (1999) 21–27.
[3] M.L.A. Pervier, Mechanics of Ice Detachment Applied to Turbomachinery (Ph.D. thesis), Cranfield University, 2012.
[4] E.M. Schulson, Brittle failure of ice, Eng. Fract. Mech. 68 (17–18) (2001) 1839–1887.
[5] F.D. Haynes, Effect of temperature on the strength of snow-ice, U.S. Army Cold Regions research and engineering laboratory, 1978, Corps of Engineers, CRREL Report 78-27 Hanover, New Hampshire.
[6] J.P. Dempsey, S.J. Defranco, R.M. Adamson, S.V. Mulmule, Scale effects on the in-situ tensile strength and fracture of ice, part I: Large grained freshwater ice at Spray Lakes Reservoir, Alberta, Int. J. Fract. 95 (1–4) (1999) 325–345.
[7] J.P. Dempsey, R.M. Adamson, S.V. Mulmule, Scale effects on the in-situ tensile strength and fracture of ice, part II: First-year sea ice at Resolute, NWT, Int. J. Fract. 95 (1–4) (1999) 347–366.
[8] J.H. Currier, E.M. Schulson, The tensile-strength of ice as a function of grain-size, Acta Metall. 30 (8) (1982) 1511–1514.
[9] J.J. Petrovic, Review mechanical properties of ice and snow, J. Mater. Sci. 38 (2003) 1–6.
[10] M. Aly, R. Taylor, E.Bailey. Dudley, I. Turnbull, Scale effect in ice flexural strength, J. Offshore Mech. Arct. Eng. 141 (5) (2019).
[11] J. Druez, D.D. Nguyeh, Y. Lavoie, Mechanical properties of atmospheric ice, Cold Reg. Sci. & Technol. 13 (1986) 67–74.
[12] M. Kermani, M. Farzaneh, R. Gagnon, Compressive strength of atmospheric ice, Cold Reg. Sci. & Technol. 49 (2007) 195–205.
[13] M. Kermani, M. Farzaneh, R. Gagnon, Bending strength and effective modulus of atmospheric ice, Cold Reg. Sci. & Technol. 53 (2008) 162–169.
[14] A.M.A. Mohamed, M. Farzaneh, An experimental study on the tensile properties of atmospheric ice, Cold Reg. Sci. & Technol. 68 (2011) 91–98.
[15] H. Farid, M. Farzaneh, A. Saeidi, F. Erchiqui, A contribution to the study of the compressive behavior of atmospheric ice, Cold Reg. Sci. & Technol. 121 (2016) 60–65.
[16] J.R. Stallabrass, R.D. Price, On the adhesion of ice to various materials, 1962, National research laboratories LR-350.
[17] M.C. Chu, R.J. Scavuzzo, Adhesive shear strength of impact ice, AIAA J. 29 (11) (1991).
[18] C. Blackburn, C. Laforte, J.L. Laforte, Apparatus for measuring the adhesion force of a thin ice sheet on a substrate, in: 9th International Workshop of Atmospheric Icing Structures, 2000.
[19] M.L.A. Pervier, B. Gurrutxaga Lerma, E. Piles Moncholi, D.W. Hammond, A new test apparatus to measure the adhesive shear strength of impact ice on titanium 6Al-4V alloy, Eng. Fract. Mech. 214 (212–222) (2019).
[20] Y. Han, J. Soltis, J. Palacios, Engine inlet guide vane ice impact fragmentation, AIAA J. 56 (9) (2018).
[21] K.R. Croasdale, Ice rubbling and ice interaction with offshore facilities, Cold Reg. Sci. & Technol. 76 (37–43) (2012).
[22] ML.A. Pervier, H. Pervier, D.W. Hammond, Observation of microstructures of atmospheric ice using a new replica technique, Cold Reg. Sci. & Technol. 140 (2017) 54–57.
[23] S. Timoshenko, Strength of Materials Part I Elementary Theory and Problems, second ed., D. Van Nostrand Company, 1940.
[24] S. Tozawa, Y. Taguchi, A preliminary study of scale effect on flexural strength of ice specimen, in: Proceedings of the Fifth International Offshore Mechanics and Arctic Engineering Symposium, American Society of Mechanical Engineers, 1986, pp. 336–340.
[25] J.L. Laforte, L.C. Phan, B. Felin, Microstructure of ice accretions grown on aluminium conductors, J. Clim. Appl. Meteorol. 22 (7) (1983) 1175–1189.
[26] P.J. Rye, W.C. Macklin, Crystal size in accreted ice, Q. J. R. Meteorol. Soc. 101 (1975) 207–215.
[27] M. Aly, Analysis of Scale Effect in Ice Flexural Strength (Master of Engineering thesis), Faculty of Engineering and Applied Science Memorial University of Newfoundland, 2018.
[28] G.W. Timco, S. O'Brien, Flexural strength equation for sea ice, Cold Reg. Sci. & Technol. 22 (3) (1994) 285–298.

2023-11-02

The effect of accretion temperature on microstructure and bending strength of atmospheric ice

Fallon, C.

Elsevier

Fallon C, Truyen E, Eakins D, et al., (2023) The effect of accretion temperature on microstructure and bending strength of atmospheric ice, Materials Today Communications, Volume 37, December 2023, Article Number 107461
https://doi.org/10.1016/j.mtcomm.2023.107461